

Validation Study On Upwinding Schemes For Core MHD/Turbulent Simulation

Haruki Seto,* Masatoshi Yagi*

*National Institutes for Quantum and Radiological Science and Technology, 039-3212, Rokkasho, Aomori, Japan
seto.haruki@qst.go.jp, yagi.masatoshi@qst.go.jp

Abstract - The validity of upwinding schemes for core MHD/turbulent simulation is numerically investigated by the use of a fully linearized 3-field resistive ballooning mode (RBM) model with three different discretization schemes on a convective derivative, (1) 4th order central differential (C4), (2) 4th order linear upwinding scheme (U4), (3) 3rd order weighted essentially non-oscillatory (WENO) scheme (W3). The simulations reveal that, in the cases with U4 and W3, the temporally varying upwinding direction can be unphysical nonlinear energy channels among toroidal modes and drive unphysical mode transitions even if the equation system is fully linearized theoretically. On the other hand, growth rates and eigen functions of RBM are conserved over the simulation time in the case with C4. These results show that any upwinding scheme should not be employed in the core region where nonlinear wave couplings described by convective derivatives such as the $E \times B$ flow term and the magnetic fluttering term are the fundamental nature of plasma instability and turbulence.

I. INTRODUCTION

A three-dimensional MHD/turbulence code BOUT++ [1, 2, 3, 4] is a parallel plasma fluid simulation framework which can solve arbitrary physics models with arbitrary axisymmetric magnetic configurations as initial value problems. BOUT++ code has been developed for analyzing intermittent and periodic heat and particle flux burst phenomena called as edge localized modes (ELMs) [5] with complicated geometries including x-points such as single-null and double-null divertor configurations.

Since predicting heat load on divertor plates by heat fluxes released by ELMs is one of key issues for magnetically confined fusion devices, BOUT++ employs the 3rd order weighted essentially non-oscillatory (WENO) scheme [6, 7, 8] to evaluate convective derivatives in the scrape-off layer (SOL) and divertor region with high accuracy as a default setting for ELM crash simulations. Upwinding schemes such as the WENO scheme are powerful tools to describe convection dominant transport phenomena in neutral fluids or off-resonant flows in the SOL/divertor plasmas.

In the core plasma where nonlinear wave couplings described by convective derivatives are the fundamental nature of plasma instability and turbulence, upwinding schemes, however, can introduce numerical nonlinearity via temporally changing upwinding directions which may drive unphysical wave coupling. In this paper, the validity of upwinding schemes for resonant modes in the core region is numerically investigated by linear multi-helicity simulations of resistive ballooning mode (RBM) instability with a concentric circular equilibrium with a monotonically increasing safety factor $q(r)$ with respect to the minor radius r .

The rest of this paper is organized as follows. Section 2 gives a brief description of the 3-field RBM model. In section 3, the three discretization formula applied to convective derivative are briefly introduced. Simulation results are shown in section 4 and a summary is finally given in section 5.

II. 3-FIELD RBM AND EQUILIBRIUM MODEL

A fully linearized 3-field RBM model [9] consisting the vorticity equation Eq.(1a), the energy transport equation Eq.(1b) and the generalized Ohm's law Eq.(1c) is employed,

$$\frac{\partial U_1}{\partial t} = -B_0^2 \partial_{\parallel} \frac{J_1}{B_0} + \mathbf{b}_0 \times \boldsymbol{\kappa}_0 \cdot \nabla_{\perp} p_1 + \nu \nabla_{\perp}^2 U_1, \quad (1a)$$

$$\frac{\partial p_1}{\partial t} = -\mathbf{v}_{E1} \cdot \nabla p_0 + \chi \nabla_{\perp}^2 p_1, \quad (1b)$$

$$\frac{\partial A_{\parallel 1}}{\partial t} = -\partial_{\parallel} \phi_1 + \eta J_1, \quad (1c)$$

$$\mathbf{v}_{E1} = \frac{\mathbf{b}_0 \times \nabla_{\perp} \phi_1}{B_0}, \quad U_1 = \frac{\nabla_{\perp}^2 \phi_1}{B_0}, \quad J_1 = \nabla_{\perp}^2 A_{\parallel 1},$$

$$\partial_{\parallel} = \mathbf{b}_0 \cdot \nabla, \quad \nabla_{\perp} = \nabla - \mathbf{b}_0 \mathbf{b}_0 \cdot \nabla, \quad \nabla_{\perp}^2 = \nabla \cdot \nabla_{\perp},$$

where U_1 is the perturbed vorticity, B_0 is the equilibrium magnetic field intensity, J_1 is the perturbed parallel current, \mathbf{b}_0 is the unit vector along the equilibrium magnetic field, $\boldsymbol{\kappa}_0 = \mathbf{b}_0 \cdot \nabla \mathbf{b}_0$ is the equilibrium magnetic curvature, p_1 is the perturbed pressure, $\nu = 1.0 \times 10^{-7}$ is the perpendicular viscosity, \mathbf{v}_{E1} is the perturbed $E \times B$ flow, p_0 is the equilibrium pressure, $\chi = 1.0 \times 10^{-7}$ is the perpendicular diffusivity, $A_{\parallel 1}$ is the perturbed parallel vector potential, ϕ_1 is the perturbed electrostatic potential, $\eta = 1.0 \times 10^{-6}$ is the resistivity respectively. Note that the variables in this paper are normalized by the poloidal Alfvén units with the major radius at the magnetic axis $R_{ax} = 2$ [m], the magnetic field intensity at the magnetic axis $B_{ax} = 2$ [T] and the poloidal Alfvén time $t_A = 2.05 \times 10^{-7}$ [s]. In Eqs.(1), the subscript 0 stands the equilibrium part and the subscript 1 also stands the perturbed part of physical quantity.

BOUT++ code employs a field-aligned coordinates (x, y, z) [10, 11] constructed with a local orthogonal torus (LOT) coordinates (ψ, θ, ζ) [12],

$$x = \psi, \quad y = \theta, \quad z = \zeta - \int_{\theta_0}^{\theta} \nu d\theta, \quad \nu = \frac{B_t h_{\theta}}{B_p R} \quad (2)$$

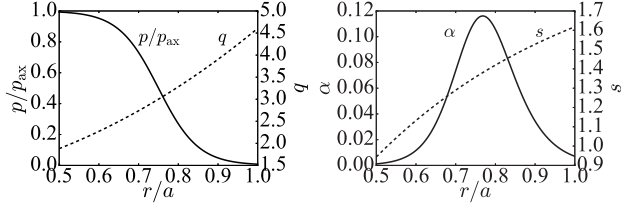


Fig. 1. The concentric circular equilibrium for RBM linear instability analyses: the radial profiles of p/p_{ax} and q (left) and the radial profiles of s and α (right), where the normalized pressure at the magnetic axis is $p_{ax} = 6.25 \times 10^{-4}$.

where x is the radial coordinate label defined by the poloidal flux function ψ , y is the parallel coordinate label defined by the orthogonal poloidal angle, z is the binormal direction label defined with the geometrical toroidal angle ζ and the local magnetic field pitch ν , B_t is the toroidal magnetic field intensity, h_θ is the poloidal arc-length, B_p is the poloidal magnetic field intensity and R is the major radius respectively. Since the field-aligned coordinates is based on the LOT coordinates (ψ, θ, ζ) to express the edge region at the vicinity of the last closed flux surface (LCFS) and the SOL region outside the LCFS, the local magnetic pitch is not constant on the flux surface. BOUT++ code, therefore, defines the safety factor as a circuit integral of the local magnetic field pitch,

$$q = \frac{1}{2\pi} \oint \nu d\theta. \quad (3)$$

When we investigate a poloidal harmonics structure of eigenfunction, we have to transform the LOT coordinates (ψ, θ, ζ) to a straight field line (SFL) coordinates (ψ, ϑ, ζ) by the use of the following relation,

$$\vartheta = \frac{1}{q} \int_0^\theta \nu(\psi, \theta_*) d\theta_*, \quad (4)$$

where this is only valid within the LCFS and q defined by Eq.(3) is therefore the safety factor in the SFL coordinates.

Fig.1 shows the concentric circular equilibrium with the pressure shear factor $\alpha \sim 0.116$ and the magnetic shear factor $s \sim 1.38$ at $r/a \sim 0.75$ used for multi-helicity RBM simulations, where $a = 0.5[\text{m}]$ is the plasma minor radius. We employ an equally-spaced grid for an $1/5$ sector of torus, i.e. $0 \leq z \leq 2\pi/5$, so that RBMs with every 5 toroidal mode numbers $n = 0, 5, 10, \dots$ can be evaluated. For a practical reason, $n = 0$ component is removed from the system and a low-pass filter $n \leq 40$ is also employed so that we take $n = 5, 10, \dots, 35, 40$ into account.

III. DISCRETIZATION FORMULA FOR CONVECTIVE DERIVATIVE

In this section, we briefly describe three differential schemes, 4th order central difference (C4) scheme, 4th order upwinding (U4) scheme and 3rd order WENO (W3) scheme employed to discretize the convective derivative $\mathbf{v}_{E1} \cdot \nabla p_0$ in Eq.(1b). The C4 scheme can be expressed by,

$$v_x \frac{\partial f}{\partial x} \rightarrow v_{x,i} \frac{-f_{i+2} + 8f_{i+1} - 8f_{i-1} + f_{i-2}}{12\Delta x}, \quad (5)$$

where the C4 scheme never selects upwinding direction so that its dispersion relation is evaluated by the same stencils with same weight factors over simulation time. The U4 scheme is a kind of ‘‘linear’’ upwinding schemes and discretizes convective derivative as,

- for $v_{x,i} > 0$,

$$v_x \frac{\partial f}{\partial x} \rightarrow v_{x,i} \frac{4f_{i+1} + 6f_i - 12f_{i-1} + 2f_{i-2}}{12\Delta x}, \quad (6a)$$

- for $v_{x,i} < 0$,

$$v_x \frac{\partial f}{\partial x} \rightarrow v_{x,i} \frac{-4f_{i-1} - 6f_i + 12f_{i+1} - 2f_{i+2}}{12\Delta x} \quad (6b)$$

where the term ‘‘linear’’ means that there is no nonlinear process to evaluate weighting factors in the U4 scheme. On the other hand, the W3 scheme is a kind of nonlinear upwinding scheme with nonlinear weighting factor w ,

- for $v_{x,i} > 0$,

$$v_x \frac{\partial f}{\partial x} \rightarrow v_{x,i} \left[\frac{f_{i+1} - f_{i-1}}{2\Delta x} - w \frac{-f_{i-2} + 3f_{i-1} - 3f_i + f_{i+1}}{2\Delta x} \right], \quad (7a)$$

$$w = \left\{ 1 + 2 \left[\frac{\epsilon + (f_i - 2f_{i-1} + f_{i-2})^2}{\epsilon + (f_{i+1} - 2f_i + f_{i-1})^2} \right]^2 \right\}^{-1}, \quad (7b)$$

- for $v_{x,i} < 0$,

$$v_x \frac{\partial f}{\partial x} \rightarrow v_{x,i} \left[\frac{f_{i+1} - f_{i-1}}{2\Delta x} - w \frac{-f_{i-1} + 3f_i - 3f_{i+1} + f_{i+2}}{2\Delta x} \right], \quad (7c)$$

$$w = \left\{ 1 + 2 \left[\frac{\epsilon + (f_{i+2} - 2f_{i+1} + f_i)^2}{\epsilon + (f_{i+1} - 2f_i + f_{i-1})^2} \right]^2 \right\}^{-1}, \quad (7d)$$

where ϵ is a small value introduced to prevent numerical singularity. Since the W3 scheme has a nonlinear weighting factor w as well as selection of the upwinding direction as possibly numerical nonlinearity sources, the U4 scheme is therefore employed to clarify whether selection of upwinding direction itself can drive unphysical mode couplings or not.

IV. SIMULATION RESULTS

Fig.2 shows the results of linear multi-helicity RBM simulations for every 5 toroidal mode numbers $n = 5, 10, \dots, 40$ with the three differential schemes. In the cases with the U4 and the W3 schemes, growth rates γ of $n = 5$ and $n = 40$ have unphysical jumps after around $t = 1000t_A$ while growth rates of all modes keep constant values in the case with the C4 scheme as shown in the column (1) of Fig.2. In addition, once unphysical mode excitations occur, their eigen functions also change from ballooning mode to interchange-like mode as shown in the columns (2)-(4) of Fig.2., although interchange mode is stable in this equilibrium. Since the unphysical mode transitions can be observed in both the U4 and the W3 schemes, it is found that selection of upwinding direction itself can be nonlinear channels and drive unphysical mode couplings.

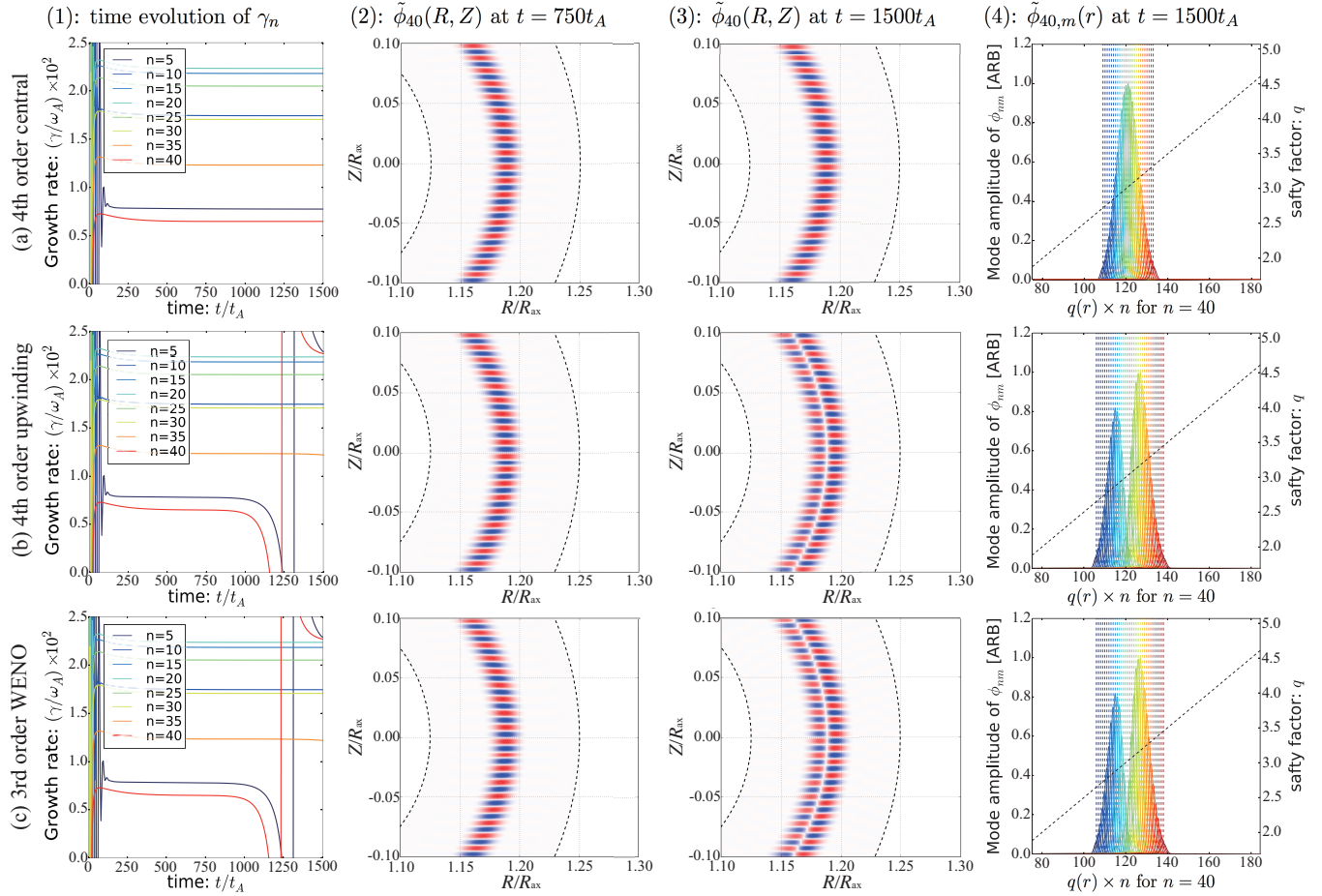


Fig. 2. Linear multi-helicity RBM analyses for every 5 toroidal mode numbers up to $n = 40$ with three differential schemes on the convective term: (a) 4th order central differential scheme, (b) 4th order upwinding scheme and (c) 3rd order WENO scheme. The column (1) shows the temporal evolution of growth rate, the column (2) shows the eigen function of $n=40$ mode of ϕ_1 on the bad curvature plane in (R, Z) at $t = 750t_A$, the column (3) shows the eigen function of $n=40$ mode of ϕ_1 at the bad curvature plane in (R, Z) at $t = 1500t_A$, and the column (4) shows the poloidal harmonics of $n=40$ mode of ϕ_1 at $t = 1500t_A$ as a function of poloidal mode number $m(r) = q(r)n$ respectively.

V. CONCLUSION

The validity of upwinding schemes for MHD/turbulent simulation in the core region has been investigated numerically by a linear multi-helicity RBM simulations with three different discretization formula on the convective derivative. The results reveal that selection of upwinding direction itself can be nonlinear channels and drive unphysical mode couplings, which means that any upwinding schemes should not be employed in the core region.

ENDNOTES

The author H.S. would like to thank Dr. B.D. Dudson of University of York and Drs. X.Q. Xu and M.V. Umanisky of Lawrence Livermore National Laboratory for fruitful discussion on implementation of discretization function table in BOUT++ code. This work is partly supported by MEXT

KAKENHI Grant No. 16K18342. Computations were carried out on the Helios Super Computer at the Computational Simulation Center of the International Fusion Energy Research Centre (IFERC-CSC).

REFERENCES

1. X. Q. XU, M. V. UMANSKY, and B. DUDSON, "Boundary plasma turbulence simulations for tokamaks," *Communications in Computational Physics*, **4**, 5, 949–979 (Nov. 2008).
2. B. D. DUDSON, M. V. UMANSKY, X. Q. XU, P. B. SNYDER, and H. R. WILSON, "BOUT++: A framework for parallel plasma fluid simulations," *Computer Physics Communications*, **180**, 9, 1467–1480 (Sep. 2009).
3. X. Q. XU, B. D. DUDSON, P. B. SNYDER, M. V. UMANSKY, H. R. WILSON, and T. CASPER, "Non-

- linear ELM simulations based on a nonideal peeling–ballooning model using the BOUT++ code,” *Nuclear Fusion*, **51**, 10, 103040 (2011).
4. B. D. DUDSON, A. ALLEN, G. BREYIANNIS, E. BRUGGER, J. BUCHANAN, L. EASY, S. FARLEY, I. JOSEPH, M. KIM, A. D. MCGANN, J. T. OMOTANI, M. V. UMANSKY, N. R. WALKDEN, T. XIA, and X. Q. XU, “BOUT++: Recent and current developments,” *Journal of Plasma Physics*, **81**, 1 (001 2015).
 5. H. ZOHRM, “Edge localized modes (ELMs),” *Plasma Physics and Controlled Fusion*, **38**, 2, 105 (1996).
 6. X.-D. LIU, S. OSHER, and T. CHAN, “Weighted Essentially Non-oscillatory Schemes,” *Journal of Computational Physics*, **115**, 1, 200 – 212 (1994).
 7. G.-S. JIANG and C.-W. SHU, “Efficient Implementation of Weighted ENO Schemes,” *Journal of Computational Physics*, **126**, 1, 202 – 228 (1996).
 8. G.-S. JIANG and D. PENG, “Weighted ENO Schemes for Hamilton–Jacobi Equations,” *SIAM Journal on Scientific Computing*, **21**, 6, 2126–2143 (2000).
 9. R. D. HAZELTINE and J. D. MEISS, *Plasma Confinement*, Addison-Wesley Publishing Company (1992).
 10. A. M. DIMITS, “Fluid simulations of tokamak turbulence in quasiballooning coordinates,” *Physical Review E*, **48**, 5, 4070 (1993).
 11. M. A. BEER, S. C. COWLEY, and G. W. HAMMETT, “Field- aligned coordinates for nonlinear simulations of tokamak turbulence,” *Physics of Plasmas*, **2**, 7, 2687–2700 (1995).
 12. J. D. C. W. D. D’HAESELEER, W. N. G. HITCHON and J. L. SHOHET, *Flux Coordinates and Magnetic Field Structure*, Springer-Verlag (1991).